

Adaptive Uncoupled Matching Network Design for Compact MIMO Systems With MMSE Receiver

Yahia Hassan and Armin Wittneben

Communication Technology Laboratory, ETH Zurich, 8092 Zurich, Switzerland
 {hassan, wittneben}@nari.ee.ethz.ch

Abstract—In this paper we jointly consider the normally distinct worlds of communication system design and circuit theory. We introduce the -up to our knowledge- first algorithm to optimize the uncoupled matching network (UC-MN) at a receiver that uses a linear MMSE equalizer in a MU-MIMO system with compact antenna array at the receiver. We design our adaptive UC-MN in order to either maximize the minimum rate of all users or to maximize the total sum rate. We compare to the conventional matching, which ignores antenna coupling, and to the cases of choosing one of the MNs that either maximizes the achievable rate or maximizes the minimum user rate for joint decoding of all data streams. In all cases, we observe a considerable performance boost. We view our results as an example of the potential of jointly considering circuit theoretical aspects and communication theory, especially for systems adopting large antenna arrays in a confined space.

I. INTRODUCTION

Future wireless networks are facing several challenges. Supporting extremely high data rates, low latency and ubiquitous service are among the strongest of these challenges. Given the limitations in the available frequency resources, the use of the spatial domain seems to be the principle way to deliver such high rates. Increasing the number of antennas is known to enhance the performance. This fact led to the considerable attention that massive MIMO arrays have recently attracted [1]. Nevertheless even massive MIMO systems should be of compact size. This implies in many cases an antenna spacing of only a fraction of a wavelength (λ). These systems are referred to as *compact* MIMO systems. It is well-known that the optimum capacity achieving decoder either has to jointly decode all data streams or use streamwise decoding with successive interference cancellation [2]. The complexity and decoding delay of either type may prove prohibitive, if the number of data streams becomes large. Therefore, for massive compact MIMO systems the simple MMSE equalizer followed by a streamwise decoder, which we consider in this paper and denote by *MMSE decoder*, is of specific relevance.

Due to effects like impedance mismatch and noise correlation that result from coupling, performance of MIMO systems was shown to be dependent on the matching network (MN) design as discussed in, e.g. [3], [4]. Unfortunately, the optimal multiport MN has poor operation bandwidth [5] and is very hard to implement. Consequently, the design of the uncoupled (UC) MN gained interest. However, in the context of MIMO attention was only given to systems assuming an optimal decoder. In [6], [7] several algorithms were presented to optimize the MN given *only* the presence of the spatially

uncorrelated noise. While [6] adapts the MN for the statistical knowledge of the spatial channel, the algorithm in [7] adapts the MN for every channel realization. In [8], the MN was designed to maximize the achievable rate for a compact MIMO system in the presence of *any* noise source in case of having either instantaneous or statistical channel knowledge. In [9], for the case of having instantaneous channel knowledge, the MN was designed to maximize the minimum user rate. Design of UC-MN for systems using MMSE decoders was not done before.

In this paper, we study a multi-user (MU) MIMO scenario, with N single antenna users transmitting to one receiver with M antennas that uses an MMSE decoder. We assume full knowledge of the *instantaneous* spatial channel, for which we adapt our MN. For *any* noise contribution, we optimize the MN for two cost functions, (i) maximization of the sum rate and (ii) maximization of the minimum rate of all users. We compare our results to the cases of using the MN, which ignores the presence of coupling, and the ones, that maximize either the achievable rate or the minimum user rate given the use of an optimal decoder [2], presented in [8], [9], respectively. Our results show substantial performance enhancement when we use the matched network designed for the MMSE decoder, especially for a high number of users. Such results shed light on the potential of the cross optimization between different components of the communication system, including the RF front end components.

II. SYSTEM MODEL

We consider the uplink of a MU-MIMO system with N widely spaced *uncorrelated* and *uncoupled* single antenna users. The input-output equation relating the transmitter generator voltages \mathbf{v}_g , and the receiver load voltages \mathbf{v}_l is:

$$\mathbf{v}_l = \mathbf{A}\mathbf{v}_g + \mathbf{u}_n, \quad (1)$$

with equivalent channel matrix \mathbf{A} and noise vector \mathbf{u}_n which has the covariance matrix \mathbf{K}_n . We assume that all the users use the same power, precisely the mean of the generator voltage squared, i.e. $E[\mathbf{v}_g\mathbf{v}_g^H] = P\mathbf{I}_N$ with \mathbf{I}_N as the $N \times N$ identity matrix. In this section we summarize the relationship between the circuit components of the receiver shown in Fig.1 and the matrices \mathbf{A} and \mathbf{K}_n . Such relations were derived in [4] and extended by us in [8].

A. Circuit Components of the Receiver

The first component of the receiver is the *lossless* antenna array that has a *symmetric* coupling matrix \mathbf{Z}_{CR} . The external

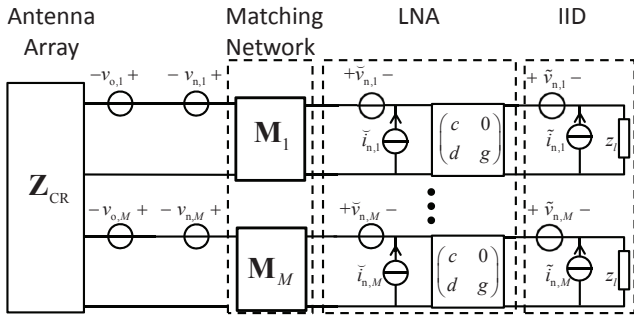


Fig. 1: Circuit model for the receiver of compact MIMO.

noise \mathbf{v}_n collected by the radiation component of the antenna array is correlated and has a noise covariance matrix \mathbf{R}_{na} which is directly proportional to the real part of \mathbf{Z}_{CR} [4].

The second component is the *lossless, reciprocal* and *purely imaginary* MN. We consider UC-MN, which means that each antenna i has its purely imaginary and reciprocal MN of impedance matrix \mathbf{M}_i . The impedance matrix \mathbf{Z}_M of the whole MN is defined as:

$$\mathbf{Z}_M = \begin{bmatrix} j\mathbf{Z}_{11} & j\mathbf{Z}_{12} \\ j\mathbf{Z}_{12} & j\mathbf{Z}_{22} \end{bmatrix}, \quad (2)$$

The v^{th} diagonal element of the diagonal matrix \mathbf{Z}_{11} denoted by $\mathbf{Z}_{11,vv}$ is equal to $\mathbf{M}_{v,11}/j$, where $\mathbf{M}_{v,11}$ is the first element of the matrix \mathbf{M}_v . The diagonal submatrices \mathbf{Z}_{12} and \mathbf{Z}_{22} are similarly constructed, but instead, $\mathbf{M}_{v,12}$ and $\mathbf{M}_{v,22}$ are used, respectively. These relations hold for any $v = 1, \dots, M$. The input impedance matrix \mathbf{Z}_R looking into the MN is:

$$\mathbf{Z}_R = j\mathbf{Z}_{11} + \mathbf{Z}_{12}(j\mathbf{Z}_{22} + \mathbf{Z}_{CR})^{-1}\mathbf{Z}_{12} = j\mathbf{Z}_{11} + \mathbf{F}_R\mathbf{Z}_{12} \quad (3)$$

The third and the fourth components of the receiver shown in Fig. 1 are the LNA and the IID parts. Each LNA has two noise sources at its input [4], a series voltage source \check{v}_n and a parallel current source \check{i}_n . The noise sources having the statistical properties $E[\check{i}_n\check{i}_n^H] = \check{\beta}\mathbf{I}_M$, $E[\check{v}_n\check{v}_n^H] = \check{\beta}\check{R}_n^2\mathbf{I}_M$ and $E[\check{v}_n\check{i}_n^H] = \check{\rho}\check{\beta}\check{R}_n\mathbf{I}_M$. The impedance matrix of the LNA is defined as $\mathbf{Z}_{LNA} = \begin{bmatrix} c & 0 \\ d & g \end{bmatrix}$. The IID part has the load impedance z_l and two noise sources, namely \tilde{v}_n and \tilde{i}_n , to account for the noise from other circuitry components that do not flow back to the antennas. They have the following characteristics, $E[\tilde{i}_n\tilde{i}_n^H] = \tilde{\beta}\mathbf{I}_M$, $E[\tilde{v}_n\tilde{v}_n^H] = \tilde{\beta}\tilde{R}_n^2\mathbf{I}_M$ and $E[\tilde{v}_n\tilde{i}_n^H] = \tilde{\rho}\tilde{\beta}\tilde{R}_n\mathbf{I}_M$.

The open circuit received voltage at the receiver antenna array \mathbf{v}_o is related to the transmitter generator voltages by

$$\mathbf{v}_o = \mathbf{Z}_{SRT}\sqrt{\alpha}\mathbf{I}_N\mathbf{v}_g, \quad (4)$$

where the scalar $\sqrt{\alpha}$ captures the effect of the circuits on the transmitters' side. The transimpedance matrix \mathbf{Z}_{SRT} resembles the physical propagation channel that maps the currents flowing in the transmitters' antennas to the voltages \mathbf{v}_o at the receiver array. We model \mathbf{Z}_{SRT} using the Kronecker model as:

$$\mathbf{Z}_{SRT} = \mathbf{R}_{RX}^{\frac{1}{2}}\mathbf{Z}_P. \quad (5)$$

The entries of the matrix \mathbf{Z}_P are independent identically distributed (i.i.d.) complex Gaussian random variables with zero mean and unit variance. The spatial correlation matrix at the receiver is denoted by \mathbf{R}_{RX} .

Using circuit theory as in [3], [4], the matrix \mathbf{A} is:

$$\mathbf{A} = j\frac{z_l d}{z_l + g}\mathbf{D}\mathbf{F}_R\mathbf{Z}_{SRT}\sqrt{\alpha} \quad (6)$$

where the matrices \mathbf{Z}_R and \mathbf{F}_R are defined in (3) and the matrix $\mathbf{D} = (c\mathbf{I}_M + \mathbf{Z}_R)^{-1}$. The covariance matrix of the noise voltages \mathbf{u}_n is given as $\mathbf{K}_n = \zeta\mathbf{D}\mathbf{\Phi}\mathbf{D}^H$, where $\zeta = |z_l d|^2 / |z_l + g|^2$ and the matrix $\mathbf{\Phi}$ defined as

$$\mathbf{\Phi} = \underbrace{\check{\beta}\left(\mathbf{Z}_R\mathbf{Z}_R^H - 2\check{R}_n\Re\{\check{\rho}^*\mathbf{Z}_R\} + \check{R}_n^2\mathbf{I}_M\right)}_{\text{LNA noise}} + \underbrace{\mathbf{F}_R\mathbf{R}_{na}\mathbf{F}_R^H}_{\text{Ant. noise}} + \underbrace{\frac{1}{|d|^2}\mathbf{D}^{-1}\psi\mathbf{I}_M\mathbf{D}^{-H}}_{\text{IID noise}}, \quad (7)$$

where $\psi = \tilde{\beta}(|g|^2 - 2\tilde{R}_n\Re\{\tilde{\rho}^*g\} + \tilde{R}_n^2)$. The complex conjugate operation is denoted by $(\cdot)^*$, while $\Re\{\cdot\}$ denotes the real part of the input argument.

B. MMSE Equalization

From classical Wiener filtering, the linear $N \times M$ filter that minimizes the mean square error between the generator voltages and the filter output is given by

$$\begin{aligned} \mathbf{G} &= \underbrace{(\mathbf{P}\mathbf{A}^H\mathbf{K}_n^{-1}\mathbf{A} + \mathbf{I}_N)^{-1}\mathbf{P}\mathbf{A}^H\mathbf{K}_n^{-1}}_{\mathbf{\Psi}} \\ &= \underbrace{(\alpha\mathbf{P}\mathbf{Z}_{SRT}^H\mathbf{F}_R^H\mathbf{\Phi}^{-1}\mathbf{F}_R\mathbf{Z}_{SRT} + \mathbf{I}_N)^{-1}\mathbf{P}\mathbf{A}^H\mathbf{K}_n^{-1}}_{\mathbf{\Psi}} \end{aligned} \quad (8)$$

The SINR per each stream i follows as

$$\gamma_i = \frac{1}{(\mathbf{\Psi}^{-1})_{ii}} - 1, \quad (9)$$

where $(\mathbf{\Psi}^{-1})_{ii}$ is the i^{th} diagonal element of the matrix $\mathbf{\Psi}^{-1}$.

III. MATCHING NETWORK OPTIMIZATION

We are going to stack the user rates in vector $\mathbf{r}_{eq} = [r_1, \dots, r_N]$, where the rate per stream i is given by

$$r_i = \log_2(1 + \gamma_i) = -\log_2((\mathbf{\Psi}^{-1})_{ii})[\text{bpcu}], \quad (10)$$

where bpcu stands for bits per channel use. Since the rate directly depends on the matrix $\mathbf{\Psi}$, this implicitly means that it depends on the choice of the MN.

If we assume full knowledge of the spatial channel \mathbf{Z}_{SRT} , we can adapt our MN to enhance the performance. We select two objective functions to maximize, the first is the sum of the user rates (MaxSR), and the second is the minimum user rate (MaxMin). We first start by defining the function $f_p(\mathbf{r}_{eq})$ which is the p norm of the vector \mathbf{r}_{eq} as,

$$f_p(\mathbf{r}_{eq}) = \left(\sum_{i=1}^N r_i^p\right)^{1/p} \quad (11)$$

An interesting property of using the f_p function of the vector of rates, is that *both* of our objective functions can be represented simply by using different p . For $p = 1$, the sum of user rates is directly obtained. If we use a *large negative* value for p , the minimum element of \mathbf{r}_{eq} will strongly dominate the sum in (11). This leads to a good approximation of the minimum component of \mathbf{r}_{eq} . Using this representation, any of the two optimization functions can be stated as

$$\begin{aligned} & \underset{\mathbf{Z}_{11}, \mathbf{Z}_{12}, \mathbf{Z}_{22}}{\text{maximize}} && f_p(\mathbf{r}_{\text{eq}}(\mathbf{Z}_{11}, \mathbf{Z}_{12}, \mathbf{Z}_{22})) \\ & \text{subject to} && \mathbf{Z}_{11}, \mathbf{Z}_{12} \text{ and } \mathbf{Z}_{22} \text{ are real and diagonal.} \end{aligned} \quad (12)$$

Where the variable p decides whether it is the MaxSR optimization or the MaxMin optimization.

To solve the optimization problems at hand, we are going to use a gradient ascend algorithm. In the following lines, we are going to derive the analytical gradient of the function in (11) with respect to the MN components. Using the matrix relations in [10], for the v^{th} diagonal element of the submatrix \mathbf{Z}_{lk} , where $\text{lk} \in \{11, 12, 22\}$, the gradient is defined as

$$\frac{\partial f_p(\mathbf{r}_{\text{eq}})}{\partial \mathbf{Z}_{\text{lk}, vv}} = \frac{1}{\ln 2} \left(\sum_{i=1}^N r_i^p \right)^{\frac{1}{p}-1} \left(\sum_{i=1}^N r_i^{p-1} \frac{-1}{(\Psi^{-1})_{ii}} \frac{\partial (\Psi^{-1})_{ii}}{\partial \mathbf{Z}_{\text{lk}, vv}} \right), \quad (13)$$

where $\frac{\partial (\Psi^{-1})_{ii}}{\partial \mathbf{Z}_{\text{lk}, vv}}$ is the i^{th} diagonal element of $\frac{\partial (\Psi^{-1})}{\partial \mathbf{Z}_{\text{lk}, vv}}$ that is

$$\frac{\partial (\Psi^{-1})}{\partial \mathbf{Z}_{\text{lk}, vv}} = -\Psi^{-1} \frac{\partial \Psi}{\partial \mathbf{Z}_{\text{lk}, vv}} \Psi^{-1}. \quad (14)$$

We define the matrix \mathbf{E}_{vv} to be the unit differential matrix with respect to the entry of the v^{th} row and v^{th} column for a diagonal matrix [10].

By inspecting (8), the partial derivative on the right hand side of (14) can be written as

$$\frac{\partial \Psi}{\partial \mathbf{Z}_{\text{lk}, vv}} = \alpha P \mathbf{Z}_{\text{SRT}}^H \left(\frac{\partial \mathbf{F}_{\text{R}}^H}{\partial \mathbf{Z}_{\text{lk}, vv}} \Phi^{-1} \mathbf{F}_{\text{R}} + \mathbf{F}_{\text{R}}^H \Phi^{-1} \frac{\partial \mathbf{F}_{\text{R}}}{\partial \mathbf{Z}_{\text{lk}, vv}} + \mathbf{F}_{\text{R}}^H \frac{\partial \Phi^{-1}}{\partial \mathbf{Z}_{\text{lk}, vv}} \mathbf{F}_{\text{R}} \right) \mathbf{Z}_{\text{SRT}}. \quad (15)$$

Note that, as discussed in [10] $\partial \mathbf{F}_{\text{R}}^H = (\partial \mathbf{F}_{\text{R}})^H$. For notational convenience we define the matrix $\mathbf{B}_1 = (j\mathbf{Z}_{22} + \mathbf{Z}_{\text{CR}})^{-1}$. Since both matrices \mathbf{Z}_{22} and \mathbf{Z}_{CR} are symmetric, \mathbf{B}_1 is also symmetric. This leads to the following partial derivatives

$$\begin{aligned} \frac{\partial \mathbf{F}_{\text{R}}}{\partial \mathbf{Z}_{12, vv}} &= \mathbf{X}_1 = \mathbf{E}_{vv} \mathbf{B}_1 \\ \frac{\partial \mathbf{F}_{\text{R}}}{\partial \mathbf{Z}_{22, vv}} &= \mathbf{X}_2 = \mathbf{F}_{\text{R}} (-j\mathbf{E}_{vv}) \mathbf{B}_1 \\ \frac{\partial \mathbf{Z}_{\text{R}}}{\partial \mathbf{Z}_{12, vv}} &= \mathbf{X}_3 = (\mathbf{X}_1 \mathbf{Z}_{12} + \mathbf{Z}_{12} \mathbf{X}_1^T) \\ \frac{\partial \mathbf{Z}_{\text{R}}}{\partial \mathbf{Z}_{22, vv}} &= \mathbf{X}_4 = \mathbf{X}_2 \mathbf{Z}_{12}. \end{aligned} \quad (16)$$

For the third partial derivative in (15),

$$\frac{\partial \Phi^{-1}}{\partial \mathbf{Z}_{\text{lk}, vv}} = -\Phi^{-1} \frac{\partial \Phi}{\partial \mathbf{Z}_{\text{lk}, vv}} \Phi^{-1}. \quad (17)$$

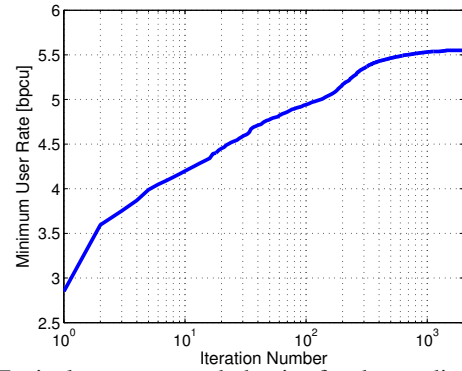


Fig. 2: Typical convergence behavior for the gradient algorithm for MaxMin optimization, $N = 10$ and $M = 30$ antennas.

We denote the LNA noise in (7) by \mathbf{T}_1 . The derivatives of \mathbf{T}_1 with respect to the MN sub-matrices are

$$\begin{aligned} \frac{\partial \mathbf{T}_1}{\partial \mathbf{Z}_{11, vv}} &= \check{\beta} j \left(\mathbf{E}_{vv} \mathbf{Z}_{\text{R}}^H - \mathbf{Z}_{\text{R}} \mathbf{E}_{vv} - \check{R}_n (\check{\rho}^* \mathbf{E}_{vv} - \check{\rho} \mathbf{E}_{vv}) \right) \\ \frac{\partial \mathbf{T}_1}{\partial \mathbf{Z}_{12, vv}} &= \check{\beta} \left(\mathbf{X}_3 \mathbf{Z}_{\text{R}}^H + \mathbf{Z}_{\text{R}} \mathbf{X}_3^H - \check{R}_n (\check{\rho}^* \mathbf{X}_3 + \check{\rho} \mathbf{X}_3^*) \right) \\ \frac{\partial \mathbf{T}_1}{\partial \mathbf{Z}_{22, vv}} &= \check{\beta} \left(\mathbf{X}_4 \mathbf{Z}_{\text{R}}^H + \mathbf{Z}_{\text{R}} \mathbf{X}_4^H - \check{R}_n (\check{\rho}^* \mathbf{X}_4 + \check{\rho} \mathbf{X}_4^*) \right). \end{aligned} \quad (18)$$

The second term in (7) is the antenna noise which we denote by \mathbf{T}_2 , whose respective derivatives are

$$\begin{aligned} \frac{\partial \mathbf{T}_2}{\partial \mathbf{Z}_{12, vv}} &= \mathbf{X}_1 \mathbf{R}_{\text{na}} \mathbf{F}_{\text{R}}^H + \mathbf{F}_{\text{R}} \mathbf{R}_{\text{na}} \mathbf{X}_1^H \\ \frac{\partial \mathbf{T}_2}{\partial \mathbf{Z}_{22, vv}} &= \mathbf{X}_2 \mathbf{R}_{\text{na}} \mathbf{F}_{\text{R}}^H + \mathbf{F}_{\text{R}} \mathbf{R}_{\text{na}} \mathbf{X}_2^H. \end{aligned} \quad (19)$$

The last term in (7) is the IID noise which we denote by \mathbf{T}_3 , and has its partial derivatives as

$$\begin{aligned} \frac{\partial \mathbf{T}_3}{\partial \mathbf{Z}_{11, vv}} &= \frac{\psi}{|d|^2} j \left(\mathbf{E}_{vv} \mathbf{D}^{-H} - \mathbf{D}^{-1} \mathbf{E}_{vv} \right) \\ \frac{\partial \mathbf{T}_3}{\partial \mathbf{Z}_{12, vv}} &= \frac{\psi}{|d|^2} \left(\mathbf{X}_3 \mathbf{D}^{-H} + \mathbf{D}^{-1} \mathbf{X}_3^H \right) \\ \frac{\partial \mathbf{T}_3}{\partial \mathbf{Z}_{22, vv}} &= \frac{\psi}{|d|^2} \left(\mathbf{X}_4 \mathbf{D}^{-H} + \mathbf{D}^{-1} \mathbf{X}_4^H \right). \end{aligned} \quad (20)$$

The gradient is then used in a conjugate gradient algorithm to find the optimal MN. We update the search direction according to the Polak-Ribiere formula discussed in [11]. We initialize the algorithm using the optimal MN for the uncoupled antennas case. The evolution of the minimum user rate as a function of the iterations for a typical channel realization is shown in Fig. 2. Even for 10 iterations, the rate of the minimum user is significantly increased.

IV. PERFORMANCE EVALUATION

In our system, the M antennas of the receiver are organized in a planar array form with minimum distance between two adjacent antennas being d_r . We consider the receiver to have $M = 30$ *parallel* antennas that are organized in two rows in the $x-y$ plane. Each row has 15 antennas. All the antennas used are half wavelength dipoles for which the coupling matrix \mathbf{Z}_{CR}

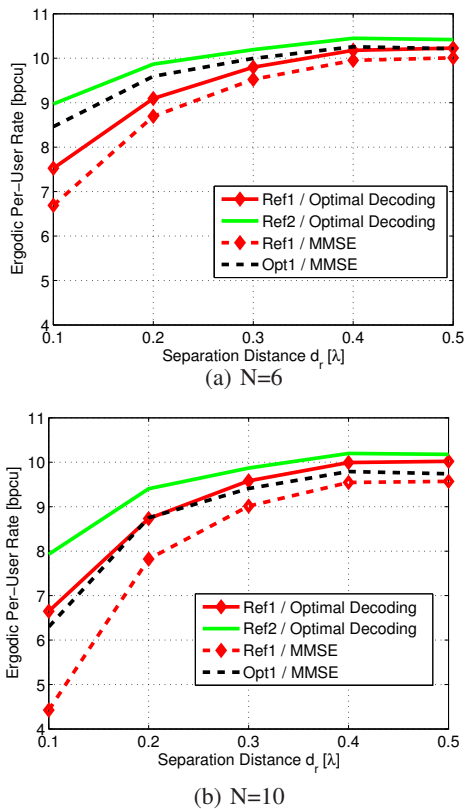


Fig. 3: Average per-user rate versus the antenna separation distance for $N = 6$ and $N = 10$ users at $\text{SNR} = 15$ dB.

can be calculated using formulas from [12]. The entries of the correlation matrix \mathbf{R}_{RX} defined in (5) are given as $\mathbf{R}_{\text{RX},ij} = J_0(2\pi d_{i,j})$, where $d_{i,j}$ is the separation between the i^{th} and j^{th} antenna, and J_0 is the first kind Bessel function of order 0. Same pathloss is assumed for all users. We assume that the LNA is the dominant noise source, i.e. in (7) $\psi \approx 0$ and $\mathbf{R}_{\text{na}} \approx 0$. The following specs of the LNA are set to: $c = \tilde{R}_n = 75\Omega$ and $\tilde{\rho} = 0$. We define the signal to noise ratio (SNR) as the average received SNR for the case $M = N = 1$.

We are going to compare the system performance for different choices of the UC-MN. Our reference cases are

- Ref1: Conventional noise matching, which is optimal for uncoupled antennas.
- Ref2: MN that maximizes the sum rate when employing an optimal decoder [8].
- Ref3: MN that maximizes the minimum user rate when employing an optimal decoder [9].

The two MNs proposed in this paper are:

- Opt1: MN that maximizes the achievable sum rate for MMSE decoder.
- Opt2: MN that maximizes the minimum rate of all users for MMSE decoder (we use $p = -20$).

A. Average Rates For Different Sum-Rate Maximizers

In Fig. 3 we study the average rate per user as a function of the antenna separation distance d_r . The solid lines refer to the optimal decoding whereas the dashed lines refer to the MMSE decoder. The legends detail the MN/decoding type for

each curve. Fig. 3 (a) is for $N = 6$ users, while 3 (b) is for $N = 10$ users. There are several interesting observations in Fig. 3. For noise matching (Ref1), the performance gap between using optimal decoding and MMSE equalization is smaller for 6 users than for 10 users. This observation holds in general in the sense that typically the gap between the optimal decoding and the MMSE decoder diminishes as the ratio of N/M drops [1]. For similar reasons in Fig. 3 (b) we note a considerable performance improvement of the MMSE decoder with noise matching (Ref1/MMSE) when the antenna spacing is doubled from 0.1λ to 0.2λ . All of this can be attributed to the fact that the MMSE decoder performs extremely bad in channels with high eigenvalue spread. Fig. 3 shows that the usage of our proposed algorithm yields great performance enhancement especially for the interesting case of $N = 10$ and $d_r = 0.1\lambda$. Comparison of (Ref1/MMSE) to (Opt1/MMSE) reveals that the average user rate increases by about 1.9 [bps] which corresponds to an increase of 42%.

B. Outage Rates and Fairness Given MMSE Decoder

Ubiquity of service is one of the main and important requirements in modern communication systems. One of the ways to measure the ubiquity, is to look at the CDFs of the minimum rate of all users. For the upcoming results, we are always going to use the *MMSE decoder*. An $m\%$ outage rate R_{MO} is defined as the rate below which the *weakest* user drops with $m\%$ probability. We study the two cases of $N = 6$ users and $N = 10$ users for antenna separation $d_r = 0.1\lambda$. We also examine the effect of dropping the knowledge of the use of an MMSE decoder and assuming an optimal decoder, i.e. using Ref2 or Ref3 MN but for an MMSE decoder.

In Fig. 4, we plot the CDFs of the minimum rate of all users for different operation SNR. We consider the 1% outage rate for $N = 6$ users which can be seen in Fig. 4(a). At $\text{SNR} = 5\text{dB}$, using the noise MN (Ref1) yields an $R_{\text{MO}} = 1.75[\text{bps}]$. We can observe that for a relatively low number of users, using *any* of the optimized MNs (Opt1 or Opt2) or Ref2 or Ref3 MN would yield a substantial performance enhancement. Using the Ref2 or Ref3 MN yields $R_{\text{MO}} \approx 2.86[\text{bps}]$, while using the Opt1 MN results in an outage rate $R_{\text{MO}} \approx 3.19[\text{bps}]$. If the Opt2 MN is used which is designed to maximize the minimum rate of all users, a maximum outage rate of $R_{\text{MO}} = 3.32[\text{bps}]$ is reached, which corresponds to a performance gain of 100%. At higher SNR, the performance increases from a minimum of $4.26[\text{bps}]$ if Ref1 matching is used to a maximum $6.72[\text{bps}]$ if Opt2 matching is used.

The most interesting results can be seen in Fig. 4(b), which show the CDFs of the minimum rates of all users for $N = 10$ for SNR of 5dB and 15dB. For SNR of 5dB, using Ref1 MN, Ref2 MN, Ref3 MN and Opt1 MN yields very bad performance of $R_{\text{MO}} \approx 0.81[\text{bps}]$, while using the Opt2 matching results in $R_{\text{MO}} \approx 1.83[\text{bps}]$. At SNR of 15dB, conventional approach of ignoring the antenna coupling (Ref1), would lead to a disastrous R_{MO} of $1.74[\text{bps}]$. However, the performance is massively enhanced if the Opt2 matching which is tailored for this specific objective, is used. This leads to a R_{MO} of

4.11[bpcu]. Note that the use of the Opt2 MN at SNR 5dB gives an outage rate slightly better than using Ref1 MN at 15dB. The strength of the cross component optimization appears evidently in the curves for SNR = 15dB. Using the Ref2 or Ref3 matching and assuming optimal decoding, could be thought at first glance as an intuitive approach to deal with compact MIMO systems. However, the use of such networks strongly degrades the performances and leads to outage rates of $R_{MO} \approx 1.31$ [bpcu] and $R_{MO} \approx 1.82$ [bpcu], respectively.

To assess the performance of the proposed algorithms from a fairness point of view, we plot the CDF of ordered rates. Due to space limitations we consider only the CDFs of the 3rd, 7th and 10th strongest rates in Fig. 5 for 10 users and SNR= 5dB. For the Opt2 MN, we can see that the 7th and the 10th strongest rates have 1% outage rates of approximately 2.28 [bpcu] and 2.86 [bpcu], respectively. This translates to a difference with the outage rate of the weakest link (in Fig. 4(b)) of around 0.54 [bpcu] and 1.12 [bpcu], respectively. While for Opt1 matching we can see the difference between the 1% outage rate of the 7th and the 10th strongest rates and the weakest rate is around 1.81 [bpcu] and 2.73 [bpcu], respectively. These results show a typical behavior of both algorithms in low and moderate SNR. The MaxSR optimization would maximize the strongest users on the price of punishing the weaker ones, while the MaxMin optimization would try to get a fair performance among all users. Note that these results show that MaxMin optimization is indeed a powerful tool as it reaches a very good fairness performance with only tweaking the impedance at the receiver side.

V. CONCLUSION

In this paper, we presented a novel approach of designing the UC-MN for coupled MIMO systems with MMSE decoders. For the cost functions of maximizing the sum of user rates (*MaxSR*) and maximizing the minimum rate of all users (*MaxMin*), we derived an analytic gradient with respect to different components of the MN. We took into account that noise can be generated from *any* source. Our results showed that the use of our proposed algorithms yield substantial performance gains, especially in the case of large number of users and low antenna separation distance. They open eyes on the fact that different performance metrics such as outage, fairness and sum rate could be massively affected by the choice of the matching network.

REFERENCES

- [1] F. Rusek *et al.*, "Scaling up MIMO: Opportunities and challenges with very large arrays," *IEEE Signal Process. Mag.*, vol. 30, no. 1, pp. 40–60, Jan. 2013.
- [2] D. Tse and P. Viswanath, *Fundamentals of wireless communication*. New York, NY, USA: Cambridge University Press, 2005.
- [3] C. P. Domizioli and B. L. Hughes, "Front-end design for compact MIMO receivers: A communication theory perspective," *IEEE Trans. Commun.*, vol. 60, no. 10, pp. 2938–2949, Oct. 2012.
- [4] M. T. Ivrlac and J. A. Nosseck, "Toward a circuit theory of communication," *IEEE Trans. Circuits Syst. I, Reg. Papers*, vol. 57-I, no. 7, pp. 1663–1683, Jul. 2010.
- [5] B. K. Lau *et al.*, "Impact of matching network on bandwidth of compact antenna arrays," *IEEE Trans. Antennas Propag.*, vol. 54, no. 11, pp. 3225–3238, Nov. 2006.

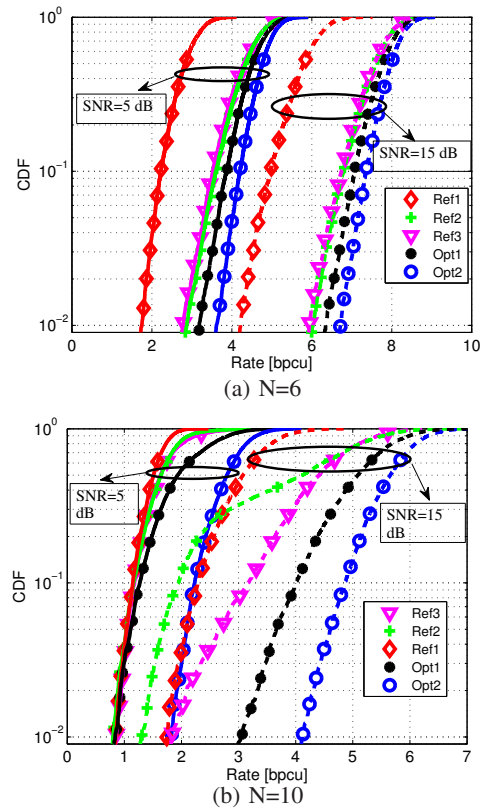


Fig. 4: Minimum rate given an MMSE equalizer for $N = 6, 10$, $M = 30$, $d_r = 0.1\lambda$ and SNR = 5, 15dB.

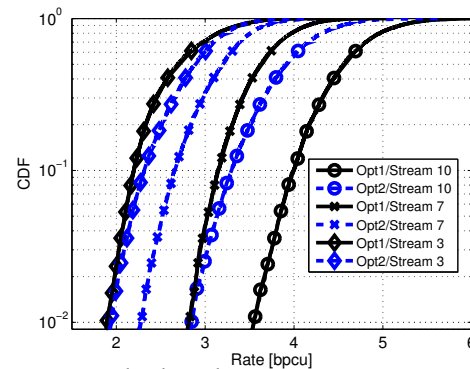


Fig. 5: CDF of (3rd, 7th, 10th) sorted rates for MMSE equalizer, $N = 10$, $M = 30$, $d_r = 0.1\lambda$ and SNR = 5dB.

- [6] Y. Fei *et al.*, "Optimal Single-Port matching impedance for capacity maximization in compact MIMO arrays," *IEEE Trans. Antennas Propag.*, vol. 56, no. 11, pp. 3566–3575, Nov. 2008.
- [7] R. Mohammadkhani and J. Thompson, "Adaptive uncoupled termination for coupled arrays in MIMO systems," *IEEE Trans. Antennas Propag.*, vol. 61, pp. 4284–4295, Aug. 2013.
- [8] Y. Hassan and A. Wittneben, "Rate maximization in coupled MIMO systems: A generic algorithm for designing single-port matching networks," in *Proc. WCNC 2014*, Istanbul, Apr. 2014.
- [9] —, "Max-min fairness in compact MU-MIMO systems: Can the matching network play a role?" in *Asilomar Conference on Signals, Systems, and Computers*, Pacific Grove, CA, USA, Nov. 2014.
- [10] K. B. Petersen and M. S. Pedersen, "The matrix cookbook," nov 2012. [Online]. Available: <http://www2.imm.dtu.dk/pubdb/p.php?3274>
- [11] J. R. Shewchuk, "An introduction to the conjugate gradient method without the agonizing pain," Pittsburgh, PA, USA, Tech. Rep., 1994.
- [12] C. Balanis, *Antenna Theory: Analysis and Design*, 3rd ed. Wiley, 2005.